Irreducible Axion Background

Kevin Langhoff,[1,2] Nadav Joseph Outmezguine,[1,2] and Nicholas L. Rodd[3]
[1]*Berkeley Center for Theoretical Physics, University of California, Berkeley, California 94720, U.S.A.*
[2]*Theory Group, Lawrence Berkeley National Laboratory, Berkeley, California 94720, U.S.A.*
[3]*Theoretical Physics Department, CERN, 1 Esplanade des Particules, CH-1211 Geneva 23, Switzerland*

(Received 19 September 2022; accepted 18 November 2022; published 5 December 2022)

Searches for dark matter decaying into photons constrain its lifetime to be many orders of magnitude larger than the age of the Universe. A corollary statement is that the abundance of any particle that can decay into photons over cosmological timescales is constrained to be much smaller than the cold dark-matter density. We show that an *irreducible* freeze-in contribution to the relic density of axions is in violation of that statement in a large portion of the parameter space. This allows us to set stringent constraints on axions in the mass range 100 eV–100 MeV. At 10 keV our constraint on a photophilic axion is $g_{a\gamma\gamma} \lesssim 8.1 \times 10^{-14}$ GeV^{-1}, almost 3 orders of magnitude stronger than the bounds established using horizontal branch stars; at 100 keV our constraint on a photophobic axion coupled to electrons is $g_{aee} \lesssim 8.0 \times 10^{-15}$, almost 4 orders of magnitude stronger than the present results. Although we focus on axions, our argument is more general and can be extended to, for instance, sterile neutrinos.

DOI: 10.1103/PhysRevLett.129.241101

The existence of an axion was first predicted to solve the problem of strong CP [1–4]; that the same particle could constitute dark matter (DM) was only realized years later [5–7]. Accordingly, experimental searches for the axion are distinguished by whether the axion is all of DM, or instead simply a state that exists in the spectrum of the Universe. The classic realization of this dichotomy is the haloscope and helioscope of Sikivie [8]. In this Letter, we consider the axions at the interface of the two paradigms. At sufficiently large couplings, axions are produced from the thermal plasma and contribute to an *irreducible* fraction of the DM density. Even when the relic density is gravitationally negligible, the strength of present constraints on DM decays can still probe this contribution and reach parameter space inaccessible to existing searches that consider stellar emission or cooling. In short, axions that do not constitute the DM of our Universe can still be strongly constrained by DM searches. We focus on axions that couple to standard model (SM) photons and electrons, through $-\frac{1}{4} g_{a\gamma\gamma} a(F\tilde{F})$ and $(g_{aee}/2m_e)(\partial_\mu a)\bar{e}\gamma^\mu\gamma_5 e$, in order to demonstrate that this argument can lead to considerably stronger bounds in the mass range 100–100 MeV. We emphasize that these are only examples of a broader observation; decaying DM searches can be highly sensitive to states that are not DM. The concept can be generalized to additional axion couplings and other light dark particles such as sterile neutrinos or dark photons.

Let us illustrate the essence of our argument with an example. For 10 keV axions that are not DM, one of the strongest constraints arises from considering anomalous energy loss from horizontal branch stars [9], and requires $g_{a\gamma\gamma} \lesssim g_{a\gamma\gamma}^{\mathrm{HB}} \equiv 6.6 \times 10^{-11}$ GeV^{-1} [11,12]. As we will establish, there exists an irreducible freeze-in contribution to the relic axion energy density ρ_a, even if the Universe only reheated to just above the temperature associated with big bang nucleosynthesis (BBN). For $m_a = 10$ keV, the relic density is approximately given by

$$\rho_a/\rho_{\mathrm{DM}} \simeq 10^{-4}(g_{a\gamma\gamma}/g_{a\gamma\gamma}^{\mathrm{HB}})^2. \tag{1}$$

Although this fraction is small, constraints on the 10 keV axion DM are strong. One of these constraints comes from observations with XMM-Newton for DM decaying to x-ray photons. These observations require $\tau_{\mathrm{DM}} \gtrsim 10^{29}\,\mathrm{s} \sim 10^{11} t_U$ at this mass [13], where t_U is the present age of the Universe. For axion DM, this implies $g_{a\gamma\gamma} \lesssim g_{a\gamma\gamma}^{\mathrm{DM}} \equiv 10^{-18}$ GeV^{-1}, almost 8 orders of magnitude smaller than $g_{a\gamma\gamma}^{\mathrm{HB}}$. If the irreducible axion contribution has a decay rate to photons of τ_a^{-1}, then to be consistent with the x-ray observations, it must satisfy $\rho_a/\tau_a \lesssim \rho_{\mathrm{DM}}/\tau_{\mathrm{DM}}$, or $\rho_a/\rho_{\mathrm{DM}} \lesssim \tau_a/\tau_{\mathrm{DM}} = (g_{a\gamma\gamma}^{\mathrm{DM}}/g_{a\gamma\gamma})^2$. Combined with Eq. (1), this requires $g_{a\gamma\gamma} \lesssim 10^{-3} g_{a\gamma\gamma}^{\mathrm{HB}}$, considerably stronger than the original bound.

The remainder of this Letter is dedicated to extending and formalizing the logic of the above argument, which will result in the constraints shown in Fig. 1 for photophilic

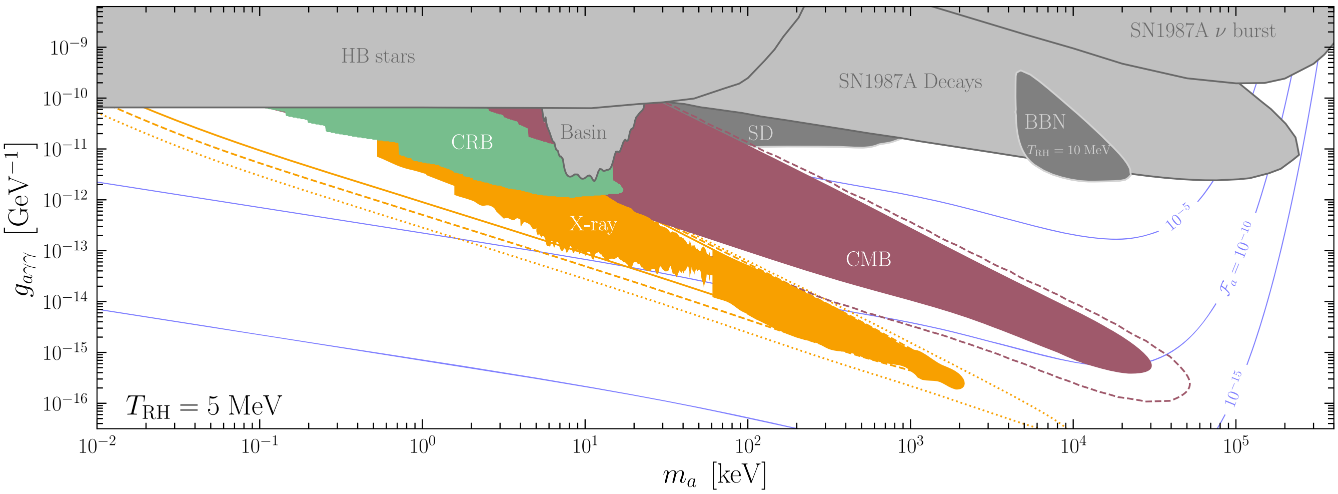

FIG. 1. Constraints on the *photophilic* axion parameters space, for the irreducible case of $T_{\rm RH} = 5$ MeV. The mustard region represents the local x-ray constraints, rescaled to the case of irreducible freeze-in axion density [13,40–46]. The sensitivity of possible future instruments on the lifetime of DM decaying locally to two photons, at the level of 10^{29}, 10^{30}, and 10^{31} s, are indicated as solid, dashed, and dotted lines respectively. (Existing searches already achieve such sensitivities at several masses.) In lime we show the parameters constrained by not overproducing the CRB [47]. The velvet region is the irreducible constraint derived from CMB anisotropies [48–51], which can be extended to the dashed region with the Simons array [50]. The dark gray region shows the irreducible constraints determined from CMB spectral distortions [52] and BBN [53] (the latter was derived for $T_{\rm RH} = 10$ MeV). The light gray regions represent astrophysical constraints on the production of axions, in horizontal branch (HB) stars [11,12] (cf. Ref. [10]), in Supernova 1987A [52,54–57], and in the Solar Basin [58]. For reference, the blue contours indicate the irreducible axion fraction $\mathcal{F}_a$.

axions ($g_{aee} = 0$) and Fig. 2 for the photophobic analog ($g_{a\gamma\gamma} = 0$). We will first outline the details of how an irreducible contribution to the axion energy density is produced in the early Universe, generalizing Eq. (1). Then, we describe how the constraints of DM can be recast to constrain these small axion energy densities. When doing so, we will consider not only late time constraints on DM decay, but also probes from earlier epochs, in particular from not overproducing the cosmic radiation background (CRB) and bounds derived from the cosmic microwave background (CMB). The need for measurements at earlier times arises for regions of parameter space where $\tau_a \ll t_U$ and the axion density in the present Universe is exponentially depleted. Details of the analysis, as well as additional and generalized constraints are shown in the Supplemental Material [14]. Specifically, we show constraints on axions that couple simultaneously to photons and electrons, the full details of our relic density calculations, and the determination of constraints when there is a misalignment contribution to the axion density. We also use sterile neutrinos as an example of the generality of the procedure of obtaining robust constraints from irreducible abundances.

The irreducible axion density.—Whenever the SM plasma contains particles that couple to axions and have energy $E \gtrsim m_a$, axions will be produced. For sufficiently large couplings, the axion will reach thermal equilibrium with the SM, which it will retain until its interaction rate drops below the rate of Hubble expansion and the axion density freezes out; this scenario is well established [62–66], understood in detail [67–71], and not our focus. Instead, we consider the scenario where axions are produced without reaching thermal equilibrium; the residual freeze-in abundance will form a relic contribution to $\rho_{\rm DM}$. Here we establish the *irreducible* contribution, leaving the observable consequences to the next section.

The higher the initial temperature of the Universe, the longer axions have to freeze in off the thermal bath, independent of whether the specific production is IR or UV dominated. We define the *reheating temperature* $T_{\rm RH}$ as the temperature of the Universe when it entered its last phase of radiation domination [72]. (We remain completely agnostic as to the state of the Universe before this—it could have been dominated by another energy source, or have not even existed.) To obtain the minimal axion abundance, we take the smallest allowed $T_{\rm RH}$, assume that at the instant of reheating $\rho_a = 0$, and compute the abundance accumulated after this time. This is *irreducible* since any assumption about the specific state of the Universe before reheating can only ever increase this abundance. The minimal reheat temperature is chosen to ensure we preserve the successes of BBN, which requires $T_{\rm RH}^{\rm min} = 5$ MeV [76–82]. An immediate implication is that any constraints obtained using this irreducible abundance will only have strength for masses up to $\mathcal{O}(100\ {\rm MeV})$ since the production of heavier axions is greatly Boltzmann suppressed.

An additional corollary of $T_{\rm RH} = 5$ MeV is that axions are produced from an epoch when only electrons, positrons,

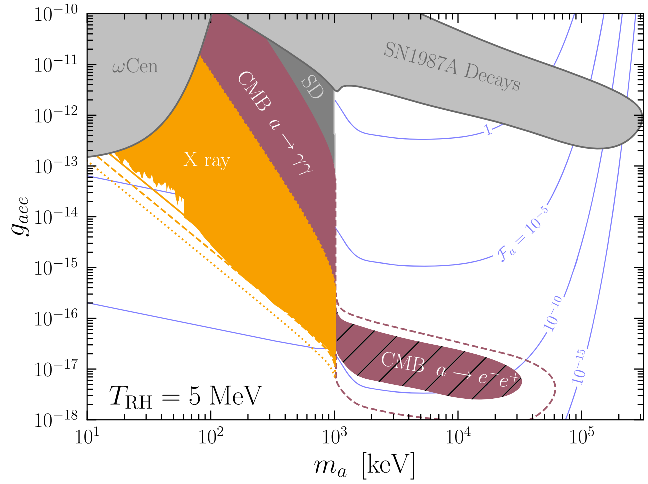

FIG. 2. The analog of Fig. 1 for a *photophobic* axion. The constraints and contours are as shown there, although here we also distinguish constraints from CMB anisotropies by whether they arise from decays to photons or electrons, with the latter shown as a black hashed region. There is a clear impact at $m_a = 2m_e$; just above threshold, the decays to e^-e^+ dominate, which shuts off the photon constraints by depleting the axion abundance. However, at lower couplings additional CMB constraints come from decays to electron-positron pairs. Light gray regions now represent prior axion constraints from Supernova 1987A [59] and red giants (RG) in the globular cluster ω Centauri [60]. (The decoupling of the RG bound with the axion mass was calculated assuming a RG core temperature of 8.6 keV [61]; the actual bound should be slightly stronger, cf. Ref. [12].)

photons, and neutrinos were in equilibrium in the SM plasma. Disregarding the neutrino coupling (cf. Ref. [83]), there are four relevant processes to consider: photon or electron-positron inverse decay ($\gamma\gamma \to a$ or $e^-e^+ \to a$), electron-positron annihilation ($e^-e^+ \to \gamma a$), and photon conversions ($e^\pm\gamma \to e^\pm a$) (cf. Ref. [52] where the photophilic irreducible abundance was considered without the inclusion of inverse decays). Having specified the processes, and a fixed $T_{\rm RH}$, we can ask what couplings would be required for the axion to achieve thermal equilibrium. For the photophobic and photophilic scenarios, the answer is furnished by $g_{a\gamma\gamma} \gtrsim 10^{-7}\ {\rm GeV}^{-1}$ [52,53,84,85] and $g_{aee} \gtrsim 10^{-9}$, respectively. For $m_a \lesssim 100$ MeV such couplings are in strong tension with a broad range of astrophysical and laboratory constraints [86]. Accordingly, freeze-in will dictate the irreducible axion density, and we confirmed that the axion never reaches equilibrium in the parameter space we constrain.

Having identified freeze-in as the relevant paradigm, we then compute the mass fraction of DM the axion constitutes as we depart from the epoch of the early Universe. Specifically, after freeze-in is completed and the axions become nonrelativistic, we can define their abundance through $\rho_a = e^{-t/\tau_a}\mathcal{F}_a\rho_{\rm DM}$, where the exponential accounts for depletion via decays, and we define

$$\mathcal{F}_a = e^{t_U/\tau_a}\rho_{a,0}/\rho_{\rm DM,0} \tag{2}$$

as the fraction of DM the axions would constitute today were they absolutely stable. We determine $\mathcal{F}_a$ from the Boltzmann equation following established techniques, e.g., Refs. [52,53,55,73,84,92–100], yielding the results shown as the blue contours in Figs. 1 and 2. (These results are made publicly available [101].) Although the calculations are standard, we emphasize several points. For $m_a \lesssim T_{\rm RH}$ photon conversion dominates the production, whereas for $m_a \gtrsim T_{\rm RH}$, inverse decays are most important—annihilations are always subdominant. Amongst the processes considered, only two are UV dominated, whereby axions are produced predominantly near reheating: electron-positron annihilation and photon conversion, both as mediated by $g_{a\gamma\gamma}$ (the g_{aee} analogs are not UV dominated). In detail, for $T_{\rm RH} = 5$ MeV, we find that freeze-in is UV dominated only when $m_a \lesssim T_{\rm RH}$ and $g_{a\gamma\gamma}/{\rm GeV}^{-1} \gtrsim 350\ g_{aee}$. For UV dominated freeze in, we find that the process is effectively completed shortly after $T_{\rm RH}$, whereas for the IR dominated process appreciable production continues until $T \sim \min(m_e/10, m_a/10)$. The full details of our calculation will be provided in the Supplemental Material [14]. Nevertheless, to provide intuition for our results, for smaller masses the density for the photophilic and photophobic scenarios—identified by a superscript (γ) and (e)—are well approximated by

$$\mathcal{F}_a^{(\gamma)} \simeq 0.20\left(\frac{m_a}{\rm keV}\right)\left(\frac{g_{a\gamma\gamma}}{10^{-8}\ {\rm GeV}^{-1}}\right)^2\left(\frac{T_{\rm RH}}{5\ {\rm MeV}}\right),$$
$$\mathcal{F}_a^{(e)} \simeq 2.4\left(\frac{m_a}{\rm keV}\right)\left(\frac{g_{aee}}{10^{-10}}\right)^2. \tag{3}$$

Both results assume $m_a \lesssim T_{\rm RH}$, and the second additionally assumes $m_a < 2m_e$. We have also set $g_{\star,s} = 10.75$. We note that in accordance with the above discussion, only the photophilic density depends on $T_{\rm RH}$ as the production is UV dominated, and in fact it remains UV dominated for $T_{\rm RH}$ even well above the electroweak scale [53].

Constraints from axion decays.—So far we have determined the irreducible axion contribution to the DM density. We now turn to the question of how one could detect (or at present constrain) a potentially small fraction of $\rho_{\rm DM}$. To do so, observe that the same couplings that produce axions in the early Universe also mediate their decays in the late Universe. Indeed, for $m_a \ll m_e$,

$$\Gamma(a \to \gamma\gamma) = \frac{m_a^3}{64\pi}\left[g_{a\gamma\gamma} + \frac{\alpha g_{aee} m_a^2}{12 m_e^3 \pi}\right]^2, \tag{4}$$

where the electron coupling mediates the decay at one loop. In analogy to Eq. (3), the decay rate in the two scenarios is

$$\tau_{a\to\gamma\gamma}^{(\gamma)} \simeq 3.0\times 10^{-6} t_U \left(\frac{m_a}{\rm keV}\right)^{-3}\left(\frac{g_{a\gamma\gamma}}{10^{-8}\ {\rm GeV}^{-1}}\right)^{-2},$$
$$\tau_{a\to\gamma\gamma}^{(e)} \simeq 1.4\times 10^{10} t_U \left(\frac{m_a}{\rm keV}\right)^{-7}\left(\frac{g_{aee}}{10^{-10}}\right)^{-2}. \tag{5}$$

While the photophobic rate is slow for the chosen couplings, the significant m_a scaling implies it becomes relevant at higher masses (although as m_a approaches $2m_e$ the expression in Eq. (4) is modified [102]). See the Supplemental Material [14] for further discussion.

A sufficiently fast decay rate can compensate for a small $\mathcal{F}_a$, and render the irreducible axion detectable. Formalizing that logic, in this section we repurpose various searches for DM decay to justify the constraints shown in Figs. 1 and 2. To do so, we will assume the axions behave exactly like cold DM (CDM). There are three effects that will violate this assumption. Firstly, the lifetime of the axion could be comparable to or much shorter than the age of the Universe, i.e., $\tau_a \ll t_U$. Here τ_a refers to the lifetime when accounting for all decay modes, for the masses we consider $a \to \gamma\gamma$ and, if it is open, $a \to e^-e^+$. To account for this we have weighted $\mathcal{F}_a$ in Eq. (2) by the appropriate factor to account for exponential depletion. The second effect relates to the use of DM searches based on observations of compact objects such as the Milky Way: lighter axions can free stream and cluster less than CDM; cf. scenarios with a small warm DM (WDM) component in addition to CDM (e.g., Refs. [40,103,104]) [105]. In the context of Milky Way like halos, simulations have confirmed that indeed the WDM component will develop a core, taking on a different spatial distribution to CDM [108]. In particular, Ref. [108] quantified that a WDM component in the Milky Way will have a position dependent fraction well described by

$$\mathcal{F}_a^{\mathrm{MW}}(r) \simeq \mathcal{F}_a \times \left[1 + 0.008\left(\frac{\mathrm{keV}}{m_a}\right)^2\left(\frac{\mathrm{kpc}}{r}\right)\right]^{-1}, \quad (6)$$

which will reduce the decay flux near the Galactic Center. We found that including this effect impacted our results by less than 5% for current constraints, but did affect the future prospects for $m_a \ll \mathrm{keV}$. At present there has not been a similar study for satellite galaxies of the Milky Way, and for this reason we chose to neglect constraints from Leo T [109]. We discuss WDM effects further in the Supplemental Material [14]. Finally, as we consider axions generated from freeze-in, they will not have the same momentum distribution as a canonical thermal relic. Nevertheless, we confirmed that the axions are always nonrelativistic at the time of the decays we consider.

Turning to existing searches, we first consider constraints on DM decaying to two photons locally, for instance, in the Milky Way. These analyses search for the following differential photon flux arising from DM decays,

$$\frac{d\Phi}{dE} = \frac{D}{2\pi m_{\mathrm{DM}}\tau_{\mathrm{DM}}}\delta(E - m_{\mathrm{DM}}/2). \quad (7)$$

Here m_{DM} and τ_{DM} are the DM mass and inverse decay rate to two photons, respectively. The term on the numerator is the D factor, and is given by the DM mass column density of the observed object, integrated over the field of view for the search [$D = \int ds d\Omega\, \rho_{\mathrm{DM}}(s,\Omega)$, see, e.g., Ref. [110]]. In the absence of a detection, instruments searching for the flux in Eq. (7) interpret their results as a constraint on the minimal allowed lifetime at that mass, which we denote $\tau_{\mathrm{DM}}^{\mathrm{min}}$.

The irreducible axion relic density can also generate a flux as in Eq. (7), however, with $m_{\mathrm{DM}} \to m_a$, $\tau_{\mathrm{DM}} \to \tau_{a\to\gamma\gamma}$, and $D \to \mathcal{F}_a e^{-t_U/\tau_a} D$. We can therefore recast the DM constraints as requiring

$$\mathcal{F}_a \leq \mathcal{F}_{\mathrm{local}}^{\mathrm{max}} \equiv \frac{\tau_{a\to\gamma\gamma}}{\tau_{\mathrm{DM}}^{\mathrm{min}}} \exp\left(\frac{t_U}{\tau_a}\right). \quad (8)$$

We exploit this criterion to convert results for $\tau_{\mathrm{DM}}^{\mathrm{min}}$ into constraints on $\mathcal{F}_a$, which we then convert to bounds on the axion couplings. The constraints we draw on are derived using XMM-Newton [13,40–42], NuSTAR [43–45], and INTEGRAL [46] observations of the Milky Way, M31, and the large Magellanic cloud. Taken together, these results are collectively labeled x-ray in Figs. 1 and 2. The breakdown of specific contributions to these results is provided in the Supplemental Material [14]. The lower boundary of the constraints is set by $\tau_{a\to\gamma\gamma}/\mathcal{F}_a \sim \tau_{\mathrm{DM}}^{\mathrm{min}}$, whereas the upper boundary occurs when $\tau_a \ll t_U$, and the local density becomes exponentially suppressed below $\mathcal{F}_a$. A dramatic example of the latter effect occurs at $m_a = 2m_e$ in Fig. 2; the opening up of the $a \to e^-e^+$ channel significantly decreases τ_a.

In order to interpret how future local DM decay searches could improve these constraints, in both figures we show the sensitivity that would be attainable if we had $\tau_{\mathrm{DM}}^{\mathrm{min}}$ at the level of 10^{29}, 10^{30}, and 10^{31} s at all masses (for a discussion of future local searches, see, e.g., Refs. [111–113]). These projections incorporate the effects encapsulated in Eq. (6). Broadly, the improvement occurs at smaller couplings—again the cutoff at larger couplings is primarily set by the exponential depletion. We can probe earlier epochs by considering constraints on decays outside the Milky Way. After accounting for the optical depth [114], such decays must not overproduce the observed CRB [47], and this allows a region of lower masses and higher couplings to be excluded in Fig. 1. (In more detail, these bounds probe redshifts of $0 \lesssim z \lesssim 20$ and energies $50\ \mathrm{eV} \lesssim E_\gamma \lesssim 3\ \mathrm{keV}$, corresponding to the ultraviolet and x-ray backgrounds.)

Observations of CMB anisotropies allow us to probe decays at earlier times still. We require

$$\mathcal{F}_a \leq \mathcal{F}_{\mathrm{CMB},\gamma\gamma/e^-e^+}^{\mathrm{max}} \equiv \frac{\tau_{a\to\gamma\gamma/e^-e^+}}{\tau_{\mathrm{CMB},\gamma\gamma/e^-e^+}^{\mathrm{min}}} \exp\left(\frac{t_{\mathrm{CMB}}}{\tau_a}\right)^{2/3}, \quad (9)$$

where we distinguish between CMB constraints set on the $\gamma\gamma$ and e^-e^+ final states, and define $t_{\mathrm{CMB}} = 8.7 \times 10^{13}\ \mathrm{s} \simeq 2 \times 10^{-4} t_U$ ($z \sim 320$). The form of Eq. (9) and the value of

$t_{\rm CMB}$ were derived by fitting the conservative "on-the-spot" approximation of Ref. [49], and were confirmed to be consistent with Refs. [48,52]. The constraints which inform $\tau^{\rm min}_{{\rm CMB},\gamma\gamma/e^-e^+}$ were taken from Ref. [50], which updated Refs. [48,49] to the Planck 2018 data, and Ref. [51]. Our results label the CMB anisotropy constraints as CMB. Nevertheless, the CMB can probe energy injections at even earlier epochs through spectral distortions. We make use of the results in Ref. [52], which took advantage of the full spectral shape of the CMB, instead of the commonly used μ and y distortions alone, specifically for the irreducible photophilic axion.

Finally, let us comment on how increasing $T_{\rm RH}$ impacts our results. For a fixed $m_a \ll T_{\rm RH}$ freeze-in of the photophilic axion is UV dominated; increasing $T_{\rm RH}$ strengthens the bounds in Fig. 1, but only weakly. Recall the lower edge of these constraints is set by comparing $\tau_{a\to\gamma\gamma}/\mathcal{F}_a$ to current lifetime bounds. This quantity scales as $g_{a\gamma\gamma}^{-4}T_{\rm RH}^{-1}$, implying the bounds improve as $g_{a\gamma\gamma} \propto T_{\rm RH}^{-1/4}$. The improvement at the upper edge is weaker, as this is dictated by the onset of exponential depletion. For reference, the $T_{\rm RH} = 100$ MeV analog of Fig. 1 is included in the Supplemental Material [14]. The scaling will be modified once $T_{\rm RH} \gtrsim 100$ MeV, when muons and pions enter the SM plasma. However, including additional particles can only increase the abundance; therefore, this scaling is conservative. The effects on the photophobic axion constraints and photophilic case for $m_a \gtrsim T_{\rm RH}$ are less pronounced as they are not UV dominated.

Conclusions.—A remarkable consequence of our present understanding of the Universe is that we cannot arbitrarily decouple its different epochs. For example, states that are sufficiently strongly coupled such that they would modify the present evolution of stars will invariably have been produced in the early Universe. The present Letter has formalized this argument for axions coupled to photons and electrons, showing that in the 100 eV–100 MeV range axions will be produced sufficiently and form a detectable fraction of the DM density.

We have sought to cast our results as irreducible in the sense that we make the most conservative assumptions about the early Universe, taking the minimal $T_{\rm RH}$ consistent with BBN. This does not imply our results are free of assumptions. For one, we have adopted a conventional cosmology between BBN and today. We have assumed a minimal scenario of the axion, coupling only to photons or electrons (although we show results when both couplings are active in the Supplemental Material [14]). If the axion decays faster to neutrinos or dark sector states then the enhanced τ_a will exponentially deplete ρ_a, cutting our constraints off from above. While such decays could potentially remove our constraints, they will also remove constraints from probes such as the Solar Basin [58,115].

Let us end with several comments on extensions to the ideas we have presented. We have ignored any contribution from the misalignment mechanism. This is because any misalignment contribution would only add to the irreducible axion abundance we adopted, and so it was conservative to exclude this possibility. We discuss how one can include misalignment in the Supplemental Material [14]. Furthermore, our analysis is not restricted to axions; it can constrain any light particle which couples to the SM. Within the dark sector framework, for instance, many of the mediators commonly considered could be constrained. Two specific examples are the dark photon and sterile neutrino. In the Supplemental Material [14] we show that constraints on the latter are particularly strong. Here, the irreducible freeze-in contribution arises from the Dodelson-Widrow mechanism [116], beginning with $\rho_s = 0$ at $T_{\rm RH} = 5$ MeV [117,118]. The sterile neutrino is then detectable through its decay to an active neutrino and a photon $\nu_s \to \nu_a\gamma$.

The present work greatly benefited from conversations with Boris Bolliet, Andrea Caputo, Joshua Foster, Fred Hiskens, Kevin Kelly, Soubhik Kumar, Hongwan Liu, Toby Opferkuch, Brandon Roach, Benjamin Safdi, Tracy Slatyer, Ken Van Tilburg, and Tomer Volansky. We particularly thank Lawrence Hall and Simon Knapen for many useful comments, and discussions that inspired this work in its initial stages. In addition, we further thank Boris Bolliet, Andrea Caputo, Francesco D'Eramo, Simon Knapen, Eric Kuflik, Hongwan Liu, Tracy Slatyer, and Ken Van Tilburg for important feedback on a draft version of our work. Our work made use of the resources provided by O'Hare [119]. The work of N. J. O. was supported in part by the Zuckerman STEM Leadership Program and by the National Science Foundation (NSF) under Grant No. PHY-1915314.

[1] R. D. Peccei and H. R. Quinn, Phys. Rev. Lett. **38**, 1440 (1977).
[2] R. D. Peccei and H. R. Quinn, Phys. Rev. D **16**, 1791 (1977).
[3] S. Weinberg, Phys. Rev. Lett. **40**, 223 (1978).
[4] F. Wilczek, Phys. Rev. Lett. **40**, 279 (1978).
[5] J. Preskill, M. B. Wise, and F. Wilczek, Phys. Lett. **120B**, 127 (1983).
[6] L. F. Abbott and P. Sikivie, Phys. Lett. **120B**, 133 (1983).
[7] M. Dine and W. Fischler, Phys. Lett. **120B**, 137 (1983).
[8] P. Sikivie, Phys. Rev. Lett. **51**, 1415 (1983); **52**, 695(E) (1984).
[9] For $m_a \lesssim 10$ eV these limits were recently strengthened by a factor of ~1.4 [10], and the constraint in our mass range can likely be similarly improved.
[10] M. J. Dolan, F. J. Hiskens, and R. R. Volkas, J. Cosmol. Astropart. Phys. 10 (2022) 096.
[11] A. Ayala, I. Domínguez, M. Giannotti, A. Mirizzi, and O. Straniero, Phys. Rev. Lett. **113**, 191302 (2014).
[12] P. Carenza, O. Straniero, B. Döbrich, M. Giannotti, G. Lucente, and A. Mirizzi, Phys. Lett. B **809**, 135709 (2020).

[13] J. W. Foster, M. Kongsore, C. Dessert, Y. Park, N. L. Rodd, K. Cranmer, and B. R. Safdi, Phys. Rev. Lett. **127**, 051101 (2021).

[14] See Supplemental Material at http://link.aps.org/supplemental/10.1103/PhysRevLett.129.241101 for a full description of our analysis and further constraints, which includes Refs. [15–39].

[15] F. Calore, P. Carenza, M. Giannotti, J. Jaeckel, and A. Mirizzi, Phys. Rev. D **102**, 123005 (2020).

[16] M. A. Shifman, A. I. Vainshtein, M. B. Voloshin, and V. I. Zakharov, Sov. J. Nucl. Phys. **30**, 711 (1979).

[17] R. Essig, E. Kuflik, S. D. McDermott, T. Volansky, and K. M. Zurek, J. High Energy Phys. 11 (2013) 193.

[18] R. Laha, J. B. Muñoz, and T. R. Slatyer, Phys. Rev. D **101**, 123514 (2020).

[19] A. Boyarsky, D. Malyshev, A. Neronov, and O. Ruchayskiy, Mon. Not. R. Astron. Soc. **387**, 1345 (2008).

[20] C. Dessert, N. L. Rodd, and B. R. Safdi, Science **367**, 1465 (2020).

[21] P. A. R. Ade *et al.* (Planck Collaboration), Astron. Astrophys. **594**, A13 (2016).

[22] M. Gorghetto, E. Hardy, and G. Villadoro, J. High Energy Phys. 07 (2018) 151.

[23] M. Gorghetto, E. Hardy, and G. Villadoro, SciPost Phys. **10**, 050 (2021).

[24] M. Buschmann, J. W. Foster, and B. R. Safdi, Phys. Rev. Lett. **124**, 161103 (2020).

[25] M. Dine, N. Fernandez, A. Ghalsasi, and H. H. Patel, J. Cosmol. Astropart. Phys. 11 (2021) 041.

[26] M. Buschmann, J. W. Foster, A. Hook, A. Peterson, D. E. Willcox, W. Zhang, and B. R. Safdi, Nat. Commun. **13**, 1049 (2022).

[27] N. Blinov, M. J. Dolan, P. Draper, and J. Kozaczuk, Phys. Rev. D **100**, 015049 (2019).

[28] J. W. Foster, S. Kumar, B. R. Safdi, and Y. Soreq, arXiv:2208.10504.

[29] P. Panci, D. Redigolo, T. Schwetz, and R. Ziegler, arXiv:2209.03371.

[30] P. B. Pal and L. Wolfenstein, Phys. Rev. D **25**, 766 (1982).

[31] X.-D. Shi and G. M. Fuller, Phys. Rev. Lett. **82**, 2832 (1999).

[32] P. D. Bolton, F. F. Deppisch, and P. S. Bhupal Dev, J. High Energy Phys. 03 (2020) 170.

[33] J. N. Abdurashitov *et al.*, Pis'ma Zh. Eksp. Teor. Fiz. **105**, 723 (2017).

[34] E. Holzschuh, W. Kündig, L. Palermo, H. Stüssi, and P. Wenk, Phys. Lett. B **451**, 247 (1999).

[35] E. Holzschuh, L. Palermo, H. Stüssi, and P. Wenk, Phys. Lett. B **482**, 1 (2000).

[36] S. Friedrich *et al.*, Phys. Rev. Lett. **126**, 021803 (2021).

[37] G. Bellini *et al.* (Borexino Collaboration), Phys. Rev. D **88**, 072010 (2013).

[38] A. Aguilar-Arevalo *et al.* (PIENU Collaboration), Phys. Rev. D **97**, 072012 (2018).

[39] X. Shi and G. Sigl, Phys. Lett. B **323**, 360 (1994); **324**, 516(E) (1994).

[40] A. Boyarsky, A. Neronov, O. Ruchayskiy, M. Shaposhnikov, and I. Tkachev, Phys. Rev. Lett. **97**, 261302 (2006).

[41] A. Boyarsky, J. Nevalainen, and O. Ruchayskiy, Astron. Astrophys. **471**, 51 (2007).

[42] A. Boyarsky, D. Iakubovskyi, O. Ruchayskiy, and V. Savchenko, Mon. Not. R. Astron. Soc. **387**, 1361 (2008).

[43] K. C. Y. Ng, B. M. Roach, K. Perez, J. F. Beacom, S. Horiuchi, R. Krivonos, and D. R. Wik, Phys. Rev. D **99**, 083005 (2019).

[44] B. M. Roach, K. C. Y. Ng, K. Perez, J. F. Beacom, S. Horiuchi, R. Krivonos, and D. R. Wik, Phys. Rev. D **101**, 103011 (2020).

[45] B. M. Roach, S. Rossland, K. C. Y. Ng, K. Perez, J. F. Beacom, B. W. Grefenstette, S. Horiuchi, R. Krivonos, and D. R. Wik, arXiv:2207.04572.

[46] F. Calore, A. Dekker, P. D. Serpico, and T. Siegert, arXiv:2209.06299.

[47] R. Hill, K. W. Masui, and D. Scott, Appl. Spectrosc. **72**, 663 (2018).

[48] T. R. Slatyer and C.-L. Wu, Phys. Rev. D **95**, 023010 (2017).

[49] V. Poulin, J. Lesgourgues, and P. D. Serpico, J. Cosmol. Astropart. Phys. 03 (2017) 043.

[50] J. Cang, Y. Gao, and Y.-Z. Ma, Phys. Rev. D **102**, 103005 (2020).

[51] B. Bolliet, J. Chluba, and R. Battye, Mon. Not. R. Astron. Soc. **507**, 3148 (2021).

[52] C. Balázs *et al.*, arXiv:2205.13549.

[53] S. Baumholzer, V. Brdar, and E. Morgante, J. Cosmol. Astropart. Phys. 05 (2021) 004.

[54] J. Jaeckel, P. C. Malta, and J. Redondo, Phys. Rev. D **98**, 055032 (2018).

[55] E. Masso and R. Toldra, Phys. Rev. D **52**, 1755 (1995).

[56] G. Lucente, P. Carenza, T. Fischer, M. Giannotti, and A. Mirizzi, J. Cosmol. Astropart. Phys. 12 (2020) 008.

[57] A. Caputo, H.-T. Janka, G. Raffelt, and E. Vitagliano, Phys. Rev. Lett. **128**, 221103 (2022).

[58] W. DeRocco, S. Wegsman, B. Grefenstette, J. Huang, and K. Van Tilburg, Phys. Rev. Lett. **129**, 101101 (2022).

[59] R. Z. Ferreira, M. C. D. Marsh, and E. Müller, arXiv:2205.07896.

[60] F. Capozzi and G. Raffelt, Phys. Rev. D **102**, 083007 (2020).

[61] G. G. Raffelt, Phys. Rep. **198**, 1 (1990).

[62] M. S. Turner, Phys. Rev. Lett. **59**, 2489 (1987); **60**, 1101 (E) (1988).

[63] S. Chang and K. Choi, Phys. Lett. B **316**, 51 (1993).

[64] E. Masso, F. Rota, and G. Zsembinszki, Phys. Rev. D **66**, 023004 (2002).

[65] S. Hannestad, A. Mirizzi, and G. Raffelt, J. Cosmol. Astropart. Phys. 07 (2005) 002.

[66] P. Graf and F. D. Steffen, Phys. Rev. D **83**, 075011 (2011).

[67] A. Salvio, A. Strumia, and W. Xue, J. Cosmol. Astropart. Phys. 01 (2014) 011.

[68] R. Z. Ferreira and A. Notari, Phys. Rev. Lett. **120**, 191301 (2018).

[69] F. Arias-Aragón, F. D'Eramo, R. Z. Ferreira, L. Merlo, and A. Notari, J. Cosmol. Astropart. Phys. 03 (2021) 090.

[70] F. D'Eramo, F. Hajkarim, and S. Yun, Phys. Rev. Lett. **128**, 152001 (2022).

[71] F. D'Eramo, F. Hajkarim, and S. Yun, J. High Energy Phys. 10 (2021) 224.
[72] The importance of T_{RH} in axion cosmology is well appreciated, see e.g. Refs. [52,73–75].
[73] P. F. Depta, M. Hufnagel, and K. Schmidt-Hoberg, J. Cosmol. Astropart. Phys. 05 (2020) 009.
[74] D. Grin, T. L. Smith, and M. Kamionkowski, Phys. Rev. D **77**, 085020 (2008).
[75] L. Visinelli and P. Gondolo, Phys. Rev. D **81**, 063508 (2010).
[76] T. Hasegawa, N. Hiroshima, K. Kohri, R. S. L. Hansen, T. Tram, and S. Hannestad, J. Cosmol. Astropart. Phys. 12 (2019) 012.
[77] P. F. de Salas, M. Lattanzi, G. Mangano, G. Miele, S. Pastor, and O. Pisanti, Phys. Rev. D **92**, 123534 (2015).
[78] K. Ichikawa, M. Kawasaki, and F. Takahashi, J. Cosmol. Astropart. Phys. 05 (2007) 007.
[79] K. Ichikawa, M. Kawasaki, and F. Takahashi, Phys. Rev. D **72**, 043522 (2005).
[80] S. Hannestad, Phys. Rev. D **70**, 043506 (2004).
[81] M. Kawasaki, K. Kohri, and N. Sugiyama, Phys. Rev. D **62**, 023506 (2000).
[82] M. Kawasaki, K. Kohri, and N. Sugiyama, Phys. Rev. Lett. **82**, 4168 (1999).
[83] G.-Y. Huang and N. Nath, Eur. Phys. J. C **78**, 922 (2018).
[84] D. Cadamuro and J. Redondo, J. Cosmol. Astropart. Phys. 02 (2012) 032.
[85] J. A. Dror, H. Murayama, and N. L. Rodd, Phys. Rev. D **103**, 115004 (2021).
[86] The "cosmological triangle" in the vicinity of $m_a \sim 1$ GeV and $g_{a\gamma\gamma} \sim 10^{-5}$ GeV^{-1}, see e.g. Refs. [73,84,87–90], has been closed [91].
[87] M. Millea, L. Knox, and B. D. Fields, Phys. Rev. D **92**, 023010 (2015).
[88] M. J. Dolan, T. Ferber, C. Hearty, F. Kahlhoefer, and K. Schmidt-Hoberg, J. High Energy Phys. 12 (2017) 094; 03 (2021) 190.
[89] V. Brdar, B. Dutta, W. Jang, D. Kim, I. M. Shoemaker, Z. Tabrizi, A. Thompson, and J. Yu, Phys. Rev. Lett. **126**, 201801 (2021).
[90] M. J. Dolan, F. J. Hiskens, and R. R. Volkas, J. Cosmol. Astropart. Phys. 09 (2021) 010.
[91] A. Caputo, G. Raffelt, and E. Vitagliano, Phys. Rev. D **105**, 035022 (2022).
[92] P. Gondolo and G. Gelmini, Nucl. Phys. **B360**, 145 (1991).
[93] J. Edsjo and P. Gondolo, Phys. Rev. D **56**, 1879 (1997).
[94] L. J. Hall, K. Jedamzik, J. March-Russell, and S. M. West, J. High Energy Phys. 03 (2010) 080.
[95] D. Cadamuro, S. Hannestad, G. Raffelt, and J. Redondo, J. Cosmol. Astropart. Phys. 02 (2011) 003.
[96] M. Blennow, E. Fernandez-Martínez, and B. Zaldivar, J. Cosmol. Astropart. Phys. 01 (2014) 003.
[97] F. D'Eramo, N. Fernandez, and S. Profumo, J. Cosmol. Astropart. Phys. 02 (2018) 046.
[98] F. D'Eramo, R. Z. Ferreira, A. Notari, and J. L. Bernal, J. Cosmol. Astropart. Phys. 11 (2018) 014.
[99] M. Bolz, A. Brandenburg, and W. Buchmuller, Nucl. Phys. **B606**, 518 (2001); **B790**, 336(E) (2008).
[100] D. I. Dunsky, L. J. Hall, and K. Harigaya, arXiv:2205.11540.
[101] https://github.com/nickrodd/IrreducibleAxionAbundance.
[102] M. Bauer, M. Neubert, and A. Thamm, J. High Energy Phys. 12 (2017) 044.
[103] A. Boyarsky, J. Lesgourgues, O. Ruchayskiy, and M. Viel, Phys. Rev. Lett. **102**, 201304 (2009).
[104] A. Boyarsky, J. Lesgourgues, O. Ruchayskiy, and M. Viel, J. Cosmol. Astropart. Phys. 05 (2009) 012.
[105] The constraints that exist on light axion DM being too hot if it was produced through freeze-in (see e.g. Refs. [53,106,107]) decouple for $\mathcal{F}_a \lesssim 0.1$ [106].
[106] F. D'Eramo and A. Lenoci, J. Cosmol. Astropart. Phys. 10 (2021) 045.
[107] G. Ballesteros, M. A. G. Garcia, and M. Pierre, J. Cosmol. Astropart. Phys. 03 (2021) 101.
[108] D. Anderhalden, J. Diemand, G. Bertone, A. V. Maccio, and A. Schneider, J. Cosmol. Astropart. Phys. 10 (2012) 047.
[109] D. Wadekar and Z. Wang, Phys. Rev. D **106**, 075007 (2022).
[110] M. Lisanti, S. Mishra-Sharma, N. L. Rodd, B. R. Safdi, and R. H. Wechsler, Phys. Rev. D **97**, 063005 (2018).
[111] C. Thorpe-Morgan, D. Malyshev, A. Santangelo, J. Jochum, B. Jäger, M. Sasaki, and S. Saeedi, Phys. Rev. D **102**, 123003 (2020).
[112] A. Dekker, E. Peerbooms, F. Zimmer, K. C. Y. Ng, and S. Ando, Phys. Rev. D **104**, 023021 (2021).
[113] K. K. Boddy *et al.*, J. High Energy Astrophys. **35**, 112 (2022).
[114] M. Cirelli, G. Corcella, A. Hektor, G. Hutsi, M. Kadastik, P. Panci, M. Raidal, F. Sala, and A. Strumia, J. Cosmol. Astropart. Phys. 03 (2011) 051; 10 (2012) E01.
[115] K. Van Tilburg, Phys. Rev. D **104**, 023019 (2021).
[116] S. Dodelson and L. M. Widrow, Phys. Rev. Lett. **72**, 17 (1994).
[117] G. Gelmini, E. Osoba, S. Palomares-Ruiz, and S. Pascoli, J. Cosmol. Astropart. Phys. 10 (2008) 029.
[118] G. B. Gelmini, P. Lu, and V. Takhistov, J. Cosmol. Astropart. Phys. 12 (2019) 047.
[119] C. O'Hare, cajohare/axionlimits: Axionlimits, https://cajohare.github.io/AxionLimits/ (2020).